JOURNAL OF MATERIALS SCIENCE 26 (1991) 6231–6236

Structure of nickel-doped α-FeOOH

T. ISHIKAWA, A. NAGASHIMA, K. KANDORI
School of Chemistry, Osaka University of Education, 4–88 Minamikawahori-cho, Tennoji-ku, Osaka 543, Japan

Colloidal particles of nickel-doped α-FeOOH prepared under varied conditions were characterized using transmission electron microscopy, X-ray diffraction, thermogravimetry-differential thermal analysis, Fourier transform infrared analysis, inductively coupled plasma spectroscopy and nitrogen adsorption. The unit cell dimensions of the resulting α-FeOOH slightly changed on doping with nickel. Both the total and surface hydroxyl ions decreased with increasing amounts of nickel. The nickel content in the surface layer determined by X-ray photoelectron spectroscopy was larger than the total nickel content determined by inductively coupled plasma spectroscopy. The results obtained indicate that the substitution of iron with nickel took place in the surface layer more than in the internal phase.

1. Introduction

The formation of colloidal ferric oxide hydroxides (FeOOH) has been found to be affected by the presence of various metal ions. Doping Cu^{2+} ions interferes with crystal growth of α- and γ-FeOOH at low concentrations [1, 2], but not the formation of β-FeOOH [3]. On the other hand, Mn^{2+} ions have less influence on the crystallinity of α-FeOOH compared with other divalent ions [4, 5]. Trivalent ions, such as Al^{3+} and Cr^{3+}, substitute Fe^{3+} ions of α- and γ-FeOOH crystal, forming solid solutions [6–10]. Furthermore, attempts have been made to incorporate various divalent metal ions into δ-FeOOH crystals [11, 12]. However, details of the state of the metal ions doped in ferric oxide hydroxides still seems to be uncertain, while the structure and properties of aluminium-substituted α-FeOOH have been extensively investigated. Nowadays α-FeOOH powder is an important starting material for manufacturing magnetic recording tapes and discs. It is empirically known that doping with a small amount of nickel, cobalt and zinc in α-FeOOH particles promotes the magnetic property and stability of the metal powders produced. This role of doped metal ions can be correlated with the states of these metals in α-FeOOH particles. On the other hand, ferric oxide hydroxides are the main corrosion products of iron to which metal elements such as copper and chromium are added to inhibit corrosion. Therefore, knowledge of the structure of α-FeOOH doped with metal ions is also thought to be significant in corrosion science.

The aim of the present work was to elucidate the structure of nickel-doped α-FeOOH. Doping with nickel was performed by ageing the solutions containing $Fe(NO_3)_3$ and $Ni(NO_3)_2$ under different conditions, and the resulting particles were examined by a variety of techniques.

2. Experimental procedure

2.1. Materials

25 ml 2 mol/l $Fe(NO_3)_3$ solution was added to the desired amount of 2 mol/l $Ni(NO_3)_2$ and the pH was adjusted to 12 by adding 1 mol/l NaOH solution drop by drop at room temperature. The resulting amorphous precipitates were aged in a covered polypropylene container at different temperatures from 30–100 °C for various times from 0–20 days. After ageing, the precipitates were thoroughly washed in distilled water and dried in an air oven at 70 °C. The amount of nickel added to the starting solutions was from 0–100 Ni/Fe mol %.

2.2. Methods

The morphology of the particles thus prepared was observed with a transmission electron microscope (Jeol 120X). X-ray diffraction (XRD) of the powders was done using a high-intensity diffractometer using CuK_α radiation (45 kV, 120 mA). Simultaneous thermogravimetry-differential thermal analysis (TG-DTA) curves were taken in air using a thermo-analyser. Infrared spectra in KBr were measured with a Fourier transform infrared (FTIR) spectrometer. To characterize the particle surface, the transmission spectra of self-supporting sample discs treated under 10^{-3} torr (1 torr = 133.322 Pa) at 75 °C for 1 h were also placed in a vacuum cell at room temperature. X-ray photoelectron spectra (XPS) were measured with a spectrometer using MgK_α radiation. Nickel and iron contained in the powders were assayed by inductively coupled plasma spectroscopy (ICP) by first dissolving in HCl. Specific surface area was determined by applying the BET equation to the nitrogen adsorption isotherm measured at − 196 °C with an automatic volumetric apparatus designed in our laboratory.

0022–2461/91 $03.00 + .12

Prior to the adsorption measurements the samples were outgassed *in vacuo* at 100 °C for 2 h.

3. Results and discussion

Fig. 1 shows typical transmission electron micrographs of the particles doped with different amounts of nickel at an ageing temperature and time of 30 °C and 20 days, respectively. Without doping, only acicular particles were formed as can be seen in Fig. 1a. From ICP measurements, the Ni^{2+} ions added to the starting solutions were found to be almost totally doped in the resulting particles. Increasing the amount of doped nickel led to an increase in the axial ratio of the resulting particles, and when doping was above 15 Ni/Fe mol % a few irregular small particles appeared in addition to the acicular particles as can be seen in Fig. 1c. The number of these irregular particles

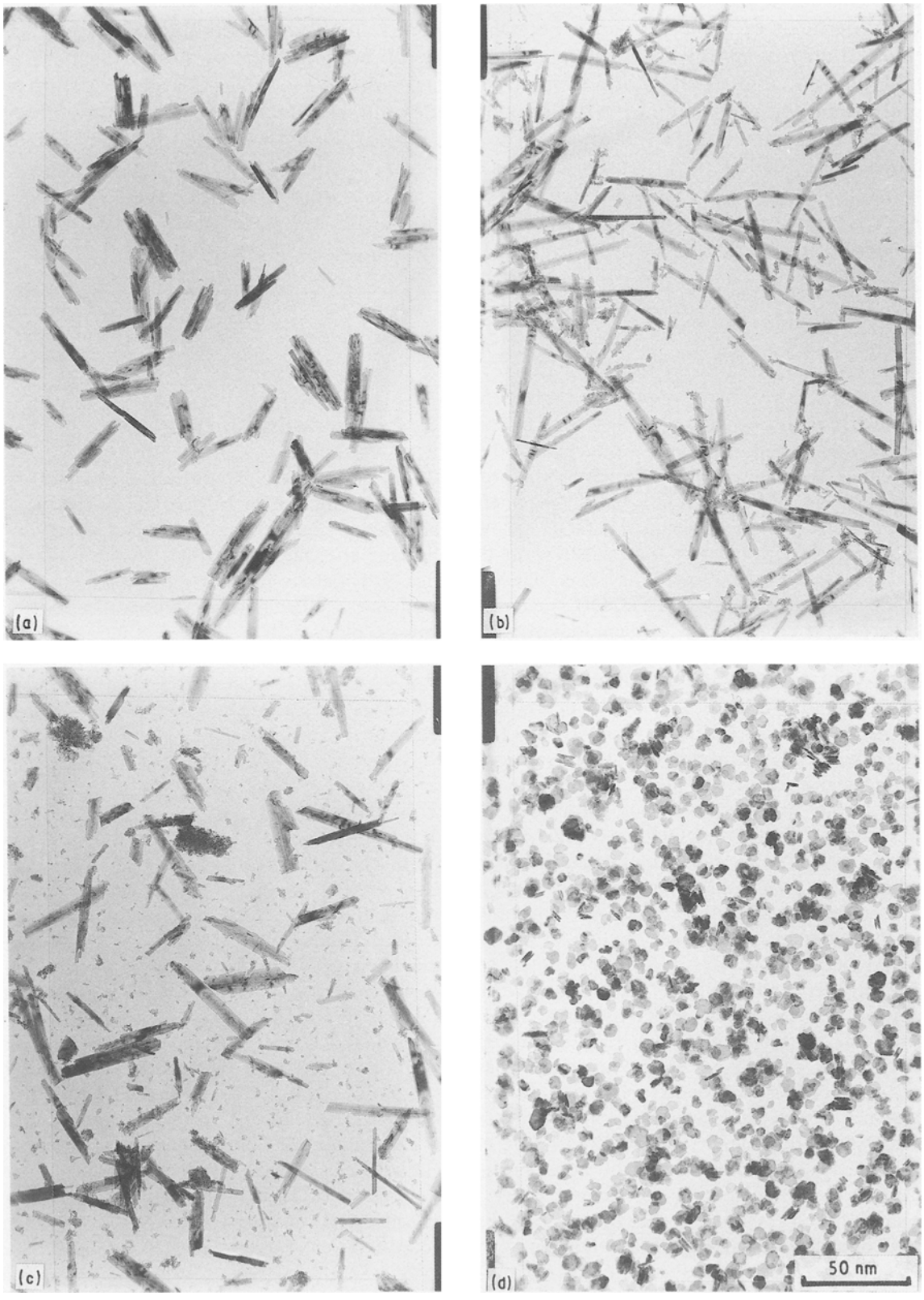

Figure 1 Transmission electron micrographs of the particles doped with different amounts of Ni^{2+} ions. The ageing temperature and time were 30 °C and 20 days, respectively. (a) Ni/Fe = 0 mol %, (b) 10 mol %, (c) 30 mol %, (d) $Ni(OH)_2$ particles.

increased with increasing amount of doped nickel. Fig. 1d shows the $Ni(OH)_2$ particles produced from the pure $Ni(NO_3)_2$ solution under the same conditions as the nickel-doped materials. These $Ni(OH)_2$ particles were platelets different from the irregular particles in Fig. 1c. The amount of doped nickel, above which the irregular particles appeared, is plotted against ageing time in Fig. 2. Below each line of this figure only acicular particles were formed. On raising the ageing temperature, the region yielding only acicular particles became narrower. When aged at 100 °C, irregular particles were always formed, even after 20 days ageing. It is considered from these results that the Ni^{2+} ions added to the starting solutions below the added amount corresponding to the lines in Fig. 2, were doped into acicular α-FeOOH particles without forming irregular particles. However, the crystal growth of α-FeOOH at a higher temperature would be too fast to incorporate Ni^{2+} ions into α-FeOOH crystals, so that irregular particles were formed.

Fig. 3 shows the XRD patterns of the materials doped with different amounts of nickel. The ageing temperature and time were 30 °C and 20 days, respectively. The patterns without doping (Fig. 3a) were characteristic of α-FeOOH and the crystallinity was slightly lowered with doping. On doping above 20%, weak additional peaks appeared as shown by the hatched peaks in Fig. 3c, and grew on increasing the doped amount. These peaks may be characteristic of the irregular particles found in the transmission electron micrographs of the materials doped more than 20% (Fig. 1c), but which were not possible to assign. Table I gives the dimensions of the unit cell evaluated from the diffraction peaks corresponding to α-FeOOH. With increasing doped amount, the *a* dimension increased and the *b* dimension decreased while the *c* dimension remained almost constant. This result indicates that the substitution of iron by nickel took place in the α-FeOOH crystals.

Fig. 4 shows the TG-DTA curves of the materials doped with different amounts of nickel, for an ageing time and temperature of 20 days and 30 °C, respectively. The DTA curves of the pure α-FeOOH clearly showed two broad endothermic peaks at temperatures from ~ 250–300 °C. Both peaks are regarded to be due to the phase transformation from α-FeOOH to α-Fe_2O_3, while usually a single endothermic peak appears in this transformation. The appearance of these two peaks seems to be attributable to the less crystalline parts in the particles formed at lower ageing temperatures, because the materials formed at higher temperatures showed only one peak due to this transformation at 295 °C. Therefore, the peak at the lower temperature seems to be caused by the transformation of the less crystalline domains. As the amount of added nickel increased, the endothermic peaks became smaller and somewhat shifted to higher temperatures. The curve of the $Ni(OH)_2$ powder had a sharp endothermic peak at 298 °C close to the endothermic peaks observed for nickel-doped materials. This sharp peak can be assigned to the transformation from $Ni(OH)_2$ to NiO, because the powder treated above this peak temperature showed an XRD pattern characteristic of NiO and the weight loss at the temperature of this peak was equal to the theoretical one conforming to the dehydroxylation reaction: $Ni(OH)_2 \rightarrow NiO + H_2O$.

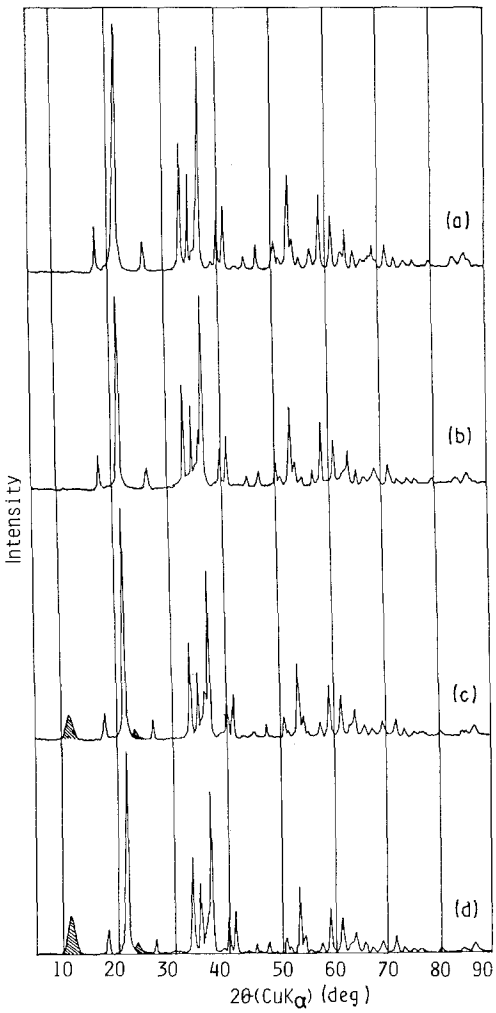

Figure 3 XRD patterns of the materials doped with various amounts of Ni^{2+} ions. The ageing time and temperature were 20 days and 30 °C, respectively. (a) Ni/Fe = 0 mol %, (b) 10 mol %, (c) 20 mol %, (d) 30 mol %. The hatched peaks could not be assigned.

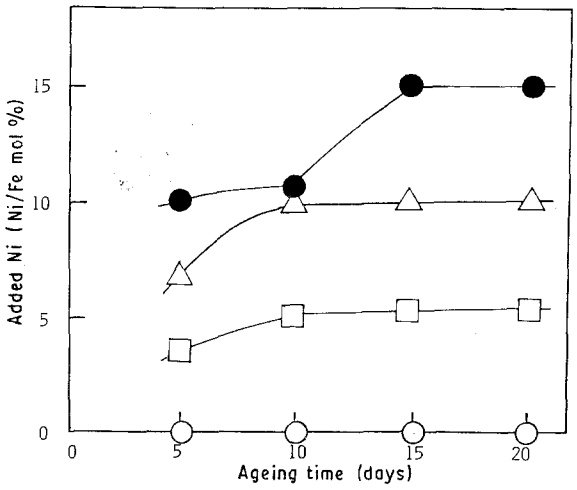

Figure 2 Relation between the ageing time and the amount of Ni^{2+} doped without forming irregular particles. Ageing temperatures: (●) 30, (△) 50, (□) 75 and (○) 100 °C.

TABLE I The amount of Ni^{2+} ions added to the starting solutions, the various nickel contents determined by ICP, XPS and infrared spectroscopy, the unit cell dimensions and the specific surface area

Added Ni (mol %)	Ni/Fe (mol %)		IR	*B*/*A*	Unit cell dimensions (nm)			Surface area ($m^2\ g^{-1}$)
	ICP (*A*)	XPS (*B*)			*a*	*b*	*c*	
0	0	0	0	–	0.996 25	0.462 52	0.302 32	65
5	–	–	12	–	–	–	–	70
10	10.3	31.9	88	3.11	0.997 20	0.462 02	0.302 37	76
20	–	–	–	–	0.997 47	0.460 01	0.302 30	173
30	29.4	59.7	96	2.03	0.998 18	0.460 85	0.302 51	194

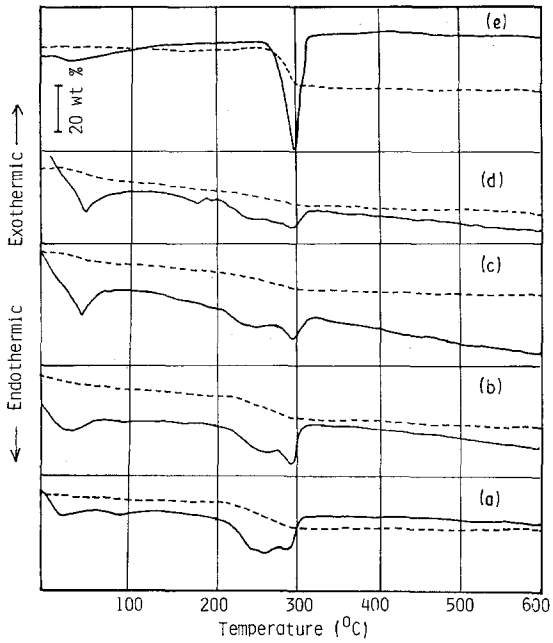

Figure 4 TG-DTA curves of the materials doped with different amounts of Ni^{2+} ions. The ageing time and temperature were 20 days and 30 °C, respectively. (——) DTA and (- - -) TG curves. (a) Ni/Fe = 0 mol %, (b) 5 mol %, (c) 10 mol %, (d) 20 mol %, (e) the $Ni(OH)_2$ particles in Fig. 1d.

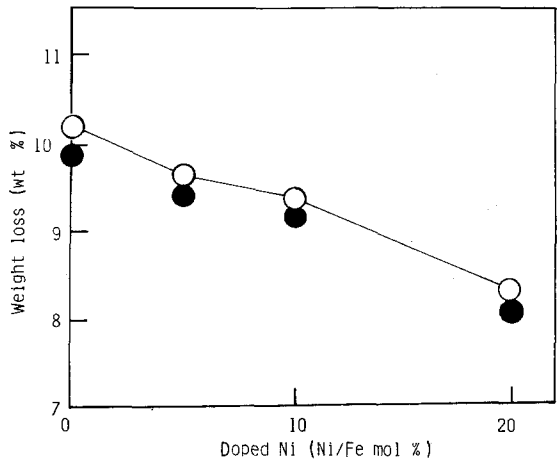

Figure 5 Relation between the weight loss caused by dehydroxylation and the amount of doped Ni^{2+} ions. The ageing time and temperature were 20 days and 30 °C, respectively. (○) Experimental and (●) theoretical weight losses.

As can be seen from the TG curves shown by the dashed lines in Fig. 4, the weight loss occurred at a temperature from 200–300 °C coinciding with those of the DTA endothermic peaks. Therefore the weight loss is regarded as being caused by the dehydroxylation reaction. Fig. 5 depicts the relation between the weight loss in the temperature range of the endothermic peak and the amount of doped nickel. The weight loss decreased with increasing doped amount, in other words, doping with nickel decreased the hydroxyl ions of the materials. According to ICP measurement, the iron content in the particles was reduced on increasing the amount of Ni^{2+} ions added to the starting solutions, this being evidence of the substitution of Fe^{3+} ions by Ni^{2+} ions in the particles. The replacement of Fe^{3+} ions with Ni^{2+} ions would result in a decrease in hydroxyl ions to maintain the charge balance, as suggested by the thermogravimetry results. Therefore, the composition formula of the nickel-doped materials is thought to be $Fe_{1-x}Ni_xO(OH)_{1-x}$, where x is the mole faction of doped nickel. The theoretical weight loss estimated from this formula was very close to the experimental weight loss. Consequently, it is plausible that the nickel-substitution led to the decrease of hydroxyl ions.

Fig. 6 shows the infrared spectra in KBr of the materials doped with different amounts of nickel for the ageing time and temperature of 20 days and 30 °C, respectively. The spectra except for Spectrum f had peaks at 895, 795, and 640 cm^{-1}. White and Roy [13] have assigned the former band to the deformation vibrations of hydroxyl ions of α-FeOOH and the latter two bands to the stretching vibrations of FeO. The broad band at 3150 cm^{-1} can be assigned to the stretching vibrations of the hydroxyl ions of α-FeOOH. Spectrum f of the $Ni(OH)_2$ materials showed two bands at 3630 and 570 cm^{-1} which can be assigned to the stretching and deformation vibrations of hydroxyl ions of $Ni(OH)_2$, respectively. The spectra of the nickel-doped materials did not show bands characteristic of $Ni(OH)_2$ even on doping with 30% Ni, hence the irregular particles detected in Fig. 1c are thought to be not $Ni(OH)_2$. The 3150 cm^{-1} band had a shoulder on the higher wave number side, which is probably due to the stretching vibrations of hydroxyl groups of water molecules adsorbed on the particle surface, because the materials doped with more than 20% Ni had a higher specific surface area, as can be seen in Table I.

The XPS spectra of the materials doped with different amounts of nickel are depicted in Fig. 7. The

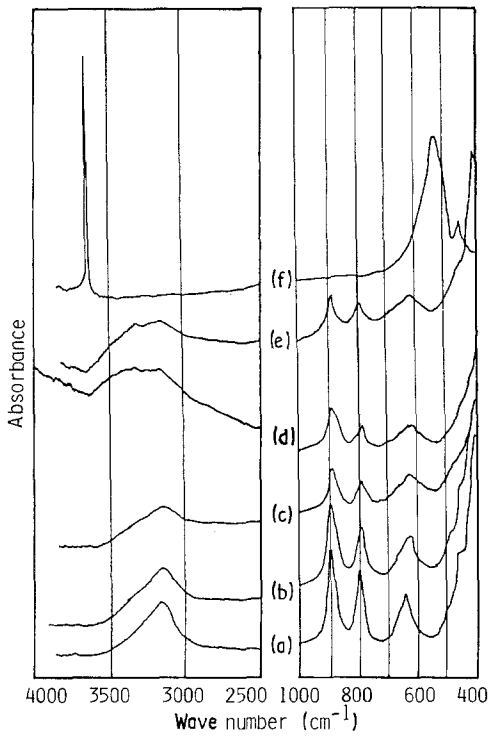

Figure 6 Transmission infrared spectra of the materials doped with various amounts of Ni^{2+} ions. The ageing time and temperature were 20 days and 30 °C, respectively. (a) Ni/Fe = 0 mol %, (b) 5 mol %, (c) 10 mol %, (d) 20 mol %, (e) 30 mol %, (f) the $Ni(OH)_2$ particles in Fig. 1d.

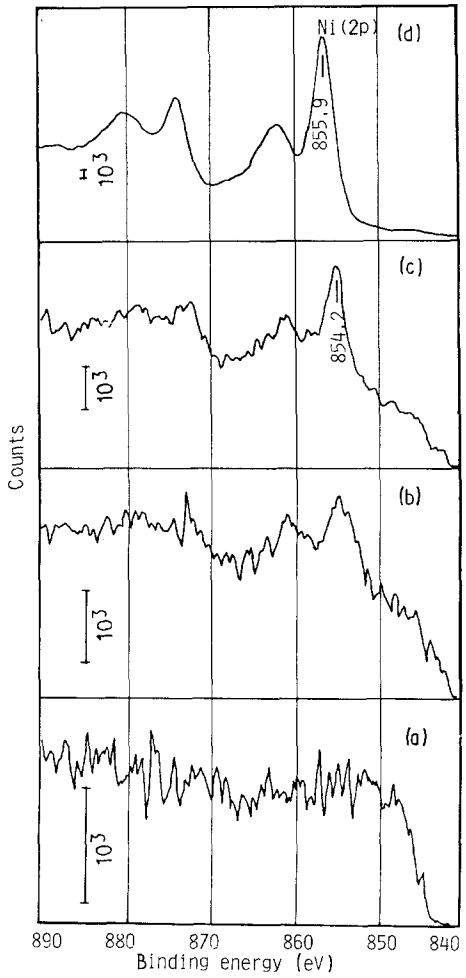

Figure 7 XPS spectra of the materials doped with different amounts of Ni^{2+} ions. The ageing time and temperature were 20 days and 30 °C. (a) Ni/Fe = 0 mol %, (b) 10 mol %, (c) 30 mol %, (d) the $Ni(OH)_2$ particles in Fig. 1d.

spectra of nickel-doped materials showed the peak of Ni(2p) at 854.2 eV, whereas the same peak of the $Ni(OH)_2$ particles appeared at 855.9 eV. This discrepancy in binding energy is significant, taking account of a resolution of 0.1 eV. This result also indicates that the doped nickel did not exist as $Ni(OH)_2$. The Ni/Fe mol % of the surface layer of particles, evaluated from the intensities of Ni(2p) and Fe(2p) peaks, is given in Table I along with that of the whole particle measured with ICP. The Ni/Fe mol % of the whole particle was smaller than that of the surface layer, although it was close to that of the starting solution. Therefore, it is evident that the doped nickel exists in the surface layer of the particles more than in the internal phase.

FTIR spectra *in vacuo* were taken to characterize the surface of nickel-doped materials. Fig. 8 shows the infrared spectra *in vacuo* of the materials doped with different amounts of nickel. Spectrum a of pure α-FeOOH had a band at 3640 cm^{-1} assigned to the stretching vibrations of the surface hydroxyl groups (Fe–OH) [14]. The absorbance of this band decreased with increasing amount of doped nickel, but this band appeared even when doped with 30% Ni. This result indicates that the surface Fe^{3+} ions were replaced by Ni^{2+} ions. It has been reported that the band of surface hydroxyl groups (Ni–OH) of NiO appears at 3676 cm^{-1} [15]. However, the spectra of the present materials did not show this band, suggesting the absence of surface Ni–OH groups. Assuming the replacement of 1 mol Fe^{3+} ion for 1 mol Ni^{2+} ion leads to the disappearance of 1 mol hydroxyl ion, the Ni/Fe

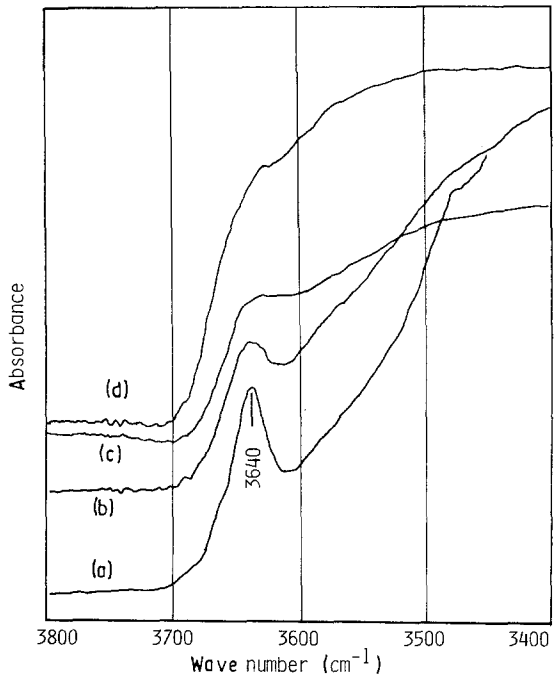

Figure 8 Transmission infrared spectra *in vacuo* of the materials doped with different amounts of Ni^{2+} ions. The ageing time and temperature were 20 days and 30 °C, respectively. (a) Ni/Fe = 0 mol %, (b) 5 mol %, (c) 10 mol %, (d) 30 mol %.

mol % of the surface can be estimated from the decrease in the absorbance of the surface Fe–OH band by doping with nickel. The surface Ni/Fe mol % thus estimated (Table I) decreased with increasing doped amount and was larger than that determined by XPS. This discrepancy in the Ni/Fe mol % determined by XPS and infrared spectroscopy can be explained in terms of the difference in the depth of the surface layer analysed by these two methods. The escape depth of photoelectrons of metal oxides is known to be from 0.3–3.0 nm [16], whereas the surface Fe–OH groups responsible for the 3640 cm^{-1} band exist just on the particle surface. So the Ni/Fe mol % determined by XPS was less than that determined by infrared spectroscopy. It can be concluded from the infrared and XPS results that the substitution of Fe^{3+} with Ni^{2+} ions occurred in the particle surface more than in the bulk phase.

References

1. K. INOUYE, S. ISHII, K. KANEKO and T. ISHIKAWA, *Z. Anorg. Allg. Chem.* **391** (1972) 86.
2. K. INOUYE, K. ICHIMURA, K. KANEKO and T. ISHIKAWA, *Corros. Sci.* **16** (1976) 507.
3. K. INOUYE, H. IMAMURA, K. KANEKO and T. ISHIKAWA, *Bull. Chem. Soc. Jpn* **47** (1974) 743.
4. T. ISHIKAWA and K. INOUYE, *Nippon Kagaku Kaishi* (1978) 665.
5. W. STIERS and U. SCHWERTMANN, *Geochim. Cosmochim. Acta* **49** (1985) 1909.
6. R. THIEL, *Z. Anorg. Allg. Chem.* **326** (1963) 70.
7. D. C. GOLDEN, L. H. BOWEN, S. B. WEED and J. M. BIGHAM, *Soil Sci. Soc. Amer. J.* **43** (1979) 802.
8. D. G. SCHULZE, *Clays Clay Miner.* **32** (1984) 36.
9. D. G. SCHULZE and U. SCHWERTMANN, *Clay Miner.* **19** (1984) 521.
10. J. MORALES, J. L. TIRADO and C. VALERA, *J. Mater. Sci.* **25** (1990) 1813.
11. S. OKAMOTO, *Kogyo Kagaku Zasshi* **67** (1967) 1855.
12. O. MULLER, R. WILSON and H. COLIJN, *J. Mater. Sci.* **15** (1980) 959.
13. W. B. WHITE and R. ROY, *Amer. Mineral.* **49** (1964) 1670.
14. T. ISHIKAWA, S. NITTA and S. KONDO, *J. Chem. Soc., Farad. Trans. 1* **80** (1984) 2033.
15. J. ERKELENS and S. H. E. BURUK, *Rec. Trav. Chim.* **92** (1972) 658.
16. C. R. BRUNDLE, *Surf. Sci.* **48** (1975) 99.

Received 6 February
and accepted 18 March 1991